

Linear and nonlinear optical investigations of polyvinyl chloride modified La₂O₃ nanocomposite films

Sultan Alhassan^{a,*}, Khulaif Alshammari^a, Majed Alshammari^a, Turki Alotaibi^a,
Alhulw H. Alshammari^a, Ali Alhamazani^a, Mohamed Henini^b, Taha Abdel Mohaymen Taha^a

^a Physics Department, College of Science, Jouf University, P.O. Box: 2014, Sakaka, Saudi Arabia

^b School of Physics and Astronomy, University of Nottingham, Nottingham NG7 2RD, UK

ARTICLE INFO

Keywords:

PVC
La₂O₃
Band gap
Refractive index
Dispersion energy

ABSTRACT

In the present work, we report the effect and improvement of PVC polymer blend nanocomposites performance with addition of lanthanum oxide (La₂O₃) nanofiller. The structural properties of the samples were studied using different characterization techniques such as XRD, FTIR, Raman and SEM. The X-ray diffraction peaks of La₂O₃ are with agreement with the pure hexagonal phase. The La₂O₃ sample was found to have crystallites size with an average about 15 nm. XRD, FTIR and SEM analysis confirmed the interaction of PVC/La₂O₃ polymer nanocomposites. The obtained band gaps of PVC/La₂O₃ polymer nanocomposites decreased (5.72 – 5.0 eV) upon increasing the nanofiller content. The obtained values of single oscillator energy (E₀) showed a decrease (5.88 – 3.28 eV) while dispersion energy (E_d) increases (5.64 – 7.20 eV) upon increasing the concentration of La₂O₃. The estimated values of static refractive index (n₀) showed an increase (1.40 – 1.79) upon increasing the percentage of La₂O₃. Moreover, the nonlinear refractive index (n₂) value was changed from 1.56 × 10⁻¹³ to 33.56 × 10⁻¹³ esu. Finally, the addition of La₂O₃ nanofillers increase the polarizability of the polymer molecules and hence the nonlinear refractive index.

Introduction

Polymer nanocomposites are a new class of materials that have attracted significant interest from both researchers and industrial scientists. This interest stems from the promising properties that these composites offer, such as enhanced mechanical, thermal, and electrical properties [1–3]. Indeed, the employment of regular and highly bright light in conjunction with polymer composites has resulted in the creation of numerous practical applications in the field of optoelectronics. These applications include sensors, devices that limit optical power, and saturable absorbers, all of which have demonstrated their significance [4,5]. Instead of resorting to costly and time-consuming procedures to identify novel monomers, it has become a standard practice to combine existing polymers to synthesis new materials which have unique properties. The ease of processing and low production cost has significantly expedited research efforts to explore new types of blends for diverse purposes. Therefore, to integrate the cost-effectiveness of organic materials with the high performance of inorganic materials, researchers have focused on developing hybrid materials, such as polymer-based

nanocomposites. Polymer matrices strengthened with nanoscale fillers are referred to as polymer nanocomposites, which represent a novel class of hybrid materials.

One of the well-known polymers is polyvinyl chloride (PVC). It is a synthetic polymer that is widely used in the manufacturing of various industrial and consumer products due to its excellent physical, chemical, and mechanical properties [6]. PVC is a type of thermoplastic polymer that is produced through the polymerization of vinyl chloride (VC) monomers. It has a high tensile strength, good chemical corrosion resistance, excellent electrical insulation properties, and is easy to process into a wide range of shapes and sizes [7–9]. PVC can also be used as a matrix in the development of polymer nanocomposites by incorporating nanofillers such as clays [10], carbon nanotubes [11], and metal oxides [12]. The resulting nanocomposites often exhibit enhanced mechanical, thermal, and optical properties compared to pure PVC or traditional PVC composites, making them valuable materials for variety of applications. However, the dispersion of nanofillers in the PVC matrix can be a challenge due to the strong interactions between the polymer and the filler, which can affect their properties and performance.

* Corresponding author.

E-mail address: ssalhassan@ju.edu.sa (S. Alhassan).

<https://doi.org/10.1016/j.rinp.2024.107456>

Received 19 September 2023; Received in revised form 17 December 2023; Accepted 5 February 2024

Available online 7 February 2024

2211-3797/© 2024 The Author(s). Published by Elsevier B.V. This is an open access article under the CC BY-NC-ND license (<http://creativecommons.org/licenses/by-nc-nd/4.0/>).

Therefore, various processing techniques have been developed to achieve improved dispersion and to optimize the properties of PVC-based nanocomposites. Furthermore, several methods including solution casting, spin coating, and dip coating which can be employed for the preparation of polymer blends. Among these methods, solvent casting stands out as the simplest and fastest for producing polymer nanocomposites. Solution casting is the most widely accessible method and does not necessitate a film processing device [13]. The structure of the resulting cast film layers is affected by the concentration of the solution. Furthermore, the thickness of the films generated by solution casting can be easily controlled by varying the amount of solution added dropwise to the Petri dishes. Recently, a study investigated by Hasan et al. [14], anatase TiO₂/PVC nanocomposites were prepared using the solution casting technique at 5 wt% and 10 wt% loading of TiO₂. The results of the study indicate a successful incorporation of TiO₂ with PVC polymer, as well as a significant enhancement in the mechanical properties of the nanocomposite when the TiO₂ loading was increased to 10 wt%, in comparison with unfilled PVC. More Recently, Gholami et al. [15] developed a composite membrane for the removal of lead heavy metals from waste waters using a casting procedure approach based on PVC-blend cellulose acetate/Fe₂O₃ NPs. Incorporating inorganic metal oxide NPs seems to be a successful method of improving PVC performance. Rare earth elements, due to their unique electron configuration, have been found to have wide-ranging applications in materials. Rare earth polymers refer to polymers that incorporate rare earth elements through physical or chemical bonding. Many functional rare earth polymers have been produced, with much of the study concentrating on luminescence, fluorescence, laser protection, optical, and magnetic properties. [16–18].

Lanthanide oxide (La₂O₃) is recognized as a cost-effective alternative in comparison to other rare earth oxides such as (Y₂O₃) and gadolinium oxide (Gd₂O₃). The incorporation of La₂O₃ nanoparticle-based nanocomposite materials has been investigated to enhance and modify the properties and performance of polymers [19,20]. Moreover, it has been found that La₂O₃ can significantly improve the abrasion resistance, while small amounts of La₂O₃ can increase thermal stability [21]. Recently, Polyvinylidene fluoride (PVDF) polymer was loaded with La₂O₃ to investigate the effect of nanofiller on the structure and crystallization of PVDF. Their studies demonstrated that the XRD analysis indicated that the addition of La₂O₃ did not modify the PVDF structure but reduced the size of its crystal structure. The Avrami equation was also used in their study to analyse isothermal crystallization, which revealed that La₂O₃ did not change the nucleation mechanism of PVDF but drastically reduced the crystallization rate [21]. Another study conducted PVC with rare earth elements like lithium triflate (LiCF₃SO₃) salt using FTIR measurement. Their results revealed that there were some overlapping and shifting of peaks in the spectra of the samples, confirming the interaction between (LiCF₃SO₃) and PVC [22]. Moreover, the synthesis of nanocomposites involved the utilization of hydrothermal and chemical methods to combine Polyaniline (PANI) nanofibers and La₂O₃ nanoparticles. To form thin films, the pure PANI and PANI/ La₂O₃ nanocomposites were deposited on n-Si and glass substrates through the spin-coating technique. Analysis of their findings indicated that the XRD pattern confirmed the crystalline properties of PANI nanofiber films and the cubic structure of PANI/ La₂O₃ films. The pure PANI films displayed a structure resembling nanofibers, while PANI/ La₂O₃ nanocomposite films showed PANI nanofibers coating La₂O₃ nanoparticles. Furthermore, their studies demonstrated that the UV–Vis spectrum of pure PANI exhibited absorption peaks at 340 and 651 nm (B and Q bands), whereas PANI/ La₂O₃ films exhibited a shift in the positions of these peaks to 320 and 620 nm. This shift indicated the occurrence of charge transfer between the PANI nanofibers and La₂O₃ nanoparticles. The optical band gap of PANI/ La₂O₃ hybrid nanocomposite films decreased as the La₂O₃ content increased from 1 to 4 vol % in the PANI nanofibers, with the B-band decreasing from 2.97 to 2.81 eV and the Q-band decreasing from 1.49 to 1.43 eV. These results led to

the conclusion that the inclusion of La₂O₃ significantly enhanced the photodetector performance of the system [23]. Additionally, S. Khound et al. conducted a study on La₂O₃ modified with polyvinyl phenol (cPVP). The key finding of this study was that a bilayer dielectric film consisting of cross-linked cPVP modified La₂O₃ improved the electrical performance of pentacene thin film transistors (TFT). Moreover, the surface properties of the La₂O₃ layer were found to enhance the growth of pentacene organic semiconductors. As a result, the on–off ratio and sub-threshold slope were significantly improved. Furthermore, the field-effect mobility of the La₂O₃/cPVP pentacene TFT was higher than that of the single-layer La₂O₃ device. This study also demonstrated the potential of integrating the rare earth oxide La₂O₃ with cPVP as a promising dielectric system for developing transistors with hybrid polymer gate dielectrics [24].

In this study, we report the impact and enhancement of PVC polymer blend nanocomposites performance through the introduction of La₂O₃ at varying concentrations (e.g., 0.3, 0.6 and 1.0 wt%). In the current investigation, the solution casting method was used to create the blend nanocomposites made of PVC-La₂O₃. The structural properties of the samples were studied using different characterization techniques such as XRD, FTIR, Ramman and SEM. The optical properties of prepared nanocomposites were also investigated.

Experimental

Analar grade PVC (MERK, Germany), tetrahydrofuran (THF) solvent supplied by CARLO ERBA and La₂O₃ nanopowder (Nanografi, Ankara, Turkey) were used to prepare PVC/La₂O₃ nanocomposite films.

The solution casting method was used to prepare the investigated samples. The first step in the preparation process is to dissolve 1.0 g of polyvinyl chloride in 30 ml of tetrahydrofuran (THF) using magnetic stirring over a room temperature period of 1.0 h. La₂O₃ was added to the PVC clear solution in increments of 0.003, 0.006, and 0.01 g, and the mixture was stirred regularly for 1.0 h. After being transferred to a glass Petri dish, the PVC/La₂O₃ combination completed room-temperature air drying. The polymer sheets, which had a thickness of around 200 μm, had been peeled off the glass plates.

For analysing the polymer films, a Shimadzu X-ray diffraction spectrometer of the model 7000 was employed, featuring CuK_{α1} radiation with a wavelength of 1.5406 Å. To conduct an ATR analysis on the polymer films, a Shimadzu FTIR-Tracer 100 was employed. The analysis revealed vibrational absorption bands corresponding to wavelengths ranging from 2000 to 399 cm⁻¹. A 785 nm Hound Unchained Labs Raman spectrometer was used for collecting the Raman signals at an exposure time of 5 s. The Thermo Fisher Quattro ESEM, an advanced environmental scanning electron microscope, is an exceptional and highly effective tool for analysing the morphology and microstructure of polymer films. Typically, before introducing the sample into the electron microscope, it is common practice to sputter a thin gold film onto the surface of the polymer film. This gold film helps enhance the conductivity and improves the quality of the imaging during the electron microscopy process. The UV–Vis optical absorption spectra of the PVC/ La₂O₃ films were recorded using the highly capable Agilent Cary 60 UV–Vis spectrophotometer.

Results and discussion

The XRD analysis was conducted to investigate the effect of La₂O₃ on PVC. The X-ray diffraction spectra of the La₂O₃, pure PVC and the PVC/ La₂O₃ polymer blend nanocomposites are shown in Fig. 1. Pure PVC exhibits peaks at 2θ ≈ 18° and 24.6°, which correspond to PVC, indicating amorphous nature (low crystallinity). After addition of La₂O₃ to polymer blend, the crystallinity of the polymer blends increased (e.g., 0.6 and 1.0 wt%), as indicated by the XRD pattern of PVC/La₂O₃ blend nanocomposites. As the loading percentage of La₂O₃ increased up to 1.0 wt%, the intensity and sharpness of peaks at 18° and 24.6° also

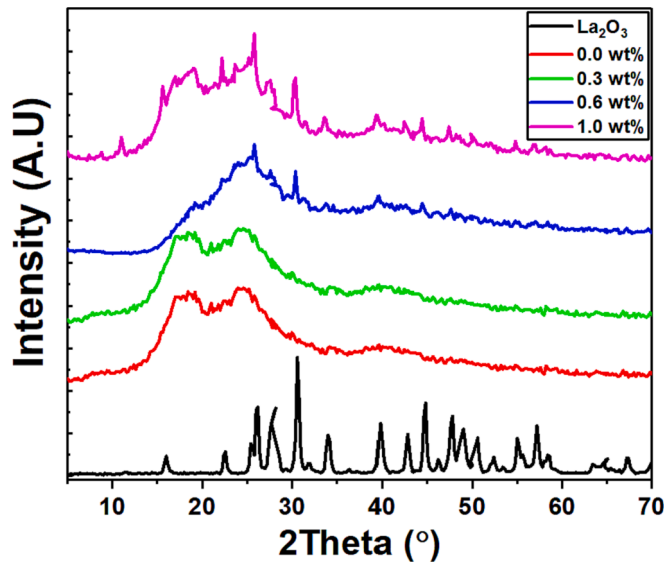


Fig. 1. XRD patterns of pure PVC, La₂O₃, and PVC-La₂O₃ nanocomposites with different concentration.

increased, suggesting an expansion in the crystalline region. As established by Hodge [25] there is a direct correlation between the degree of crystallinity and peak intensity. La₂O₃ nanoparticles can interact with the surface of the PVC chains through various forces, such as hydrogen bonding or electrostatic interactions. These interactions can restrict the mobility of the polymer chains, making it more difficult for them to crystallize. This can also contribute to a decrease in peak intensity. The observed increase in peak intensity therefore suggests an increase in the crystalline portion of PVC composites. This change can have a direct impact on the mechanical properties of PVC. The X-ray diffraction peaks of La₂O₃ are with agreement with cards (JCPDS 00-101-0278). All the peaks can be indexed to the pure hexagonal phase. The pure La₂O₃ exhibits diffraction peaks at $2\theta = 16^\circ, 26.1^\circ, 30.6^\circ, 39.8^\circ, 44.7^\circ, 46.2^\circ, 49^\circ, 52.4^\circ, 55^\circ, 63.5^\circ,$ and 67.3° , these peaks are corresponded to (hkl) with (001), (100), (10-1), (10-2), (003), (2-10), (2-11), (10-3), (2-12), (10-4), and (20-2), respectively. It is noticeable, some peaks in the samples of 6 and 10 wt% of La₂O₃ are left shifted toward lower 2θ which are may due to the increase in d spacing. It is important to notice that the presence of the peak at $2\theta = 11^\circ$ in the sample of PVC/1 wt% La₂O₃ is due to the (002) plane of La₂O₃CO₃ according to the JCPDS 00-022-0642.

The Scherrer formula was employed to determine the crystallite size diameter (D) for La₂O₃ nanocomposites all samples [26,27];

$$D = \frac{k\lambda}{\beta \cos \theta} \quad (1)$$

In the above equation, β -FWHM (full-width at half-maximum or half-width) is expressed in radians, while λ represents the X-ray wavelength of Cu_{K α 1} (1.5406 Å). The variable θ denotes the position of the diffraction peak at its maximum, and k represents the shape factor, typically assumed to be 0.9. Upon analysis, it was determined that the La₂O₃ sample exhibited crystallite sizes with an average of approximately 15 nm.

The FTIR spectrum of pure PVC and PVC-La₂O₃ nanocomposite films in the range of 400 to 4000 cm⁻¹ is shown in Fig. 2. In the pure PVC, the FTIR bands peaks observed at 609 cm⁻¹, 833 cm⁻¹, 956 cm⁻¹, 1062 cm⁻¹, 1254 cm⁻¹, 1332 cm⁻¹ and 1425 cm⁻¹. The FTIR peak of PVC polymer film at 609 cm⁻¹ is assigned to the C-Cl stretching vibration [28]. This is a strong and characteristic peak for PVC, and it is due to the presence of chlorine atoms in the PVC molecule. The chlorine atoms are attached to the carbon atoms in the backbone of the PVC chain, and they

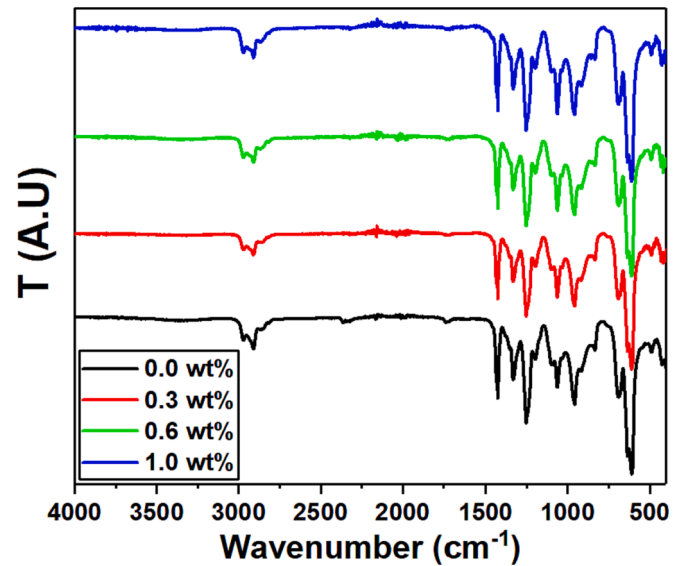


Fig. 2. FTIR spectra of pure PVC and PVC-La₂O₃ nanocomposites with different concentration.

give rise to a strong dipole moment. The rocking motion of CH₂ groups gives rise to the peak at 956 cm⁻¹. The peak at 1026 cm⁻¹ corresponds to C-C stretching, which peak indicates the vibration of the carbon atoms along the polymer backbone. The other peak at 1254 cm⁻¹ arises from the in-plane bending vibration of the hydrogen atoms in the CH₂ groups. While the peak at 1332 cm⁻¹ corresponds to the in-plane bending vibration of the hydrogen atoms in the C-H groups. Moreover, the peak located at 1425 cm⁻¹ indicates the symmetric stretching vibration of the two hydrogen atoms in the CH₂ groups [29]. Also, bands peaks observed at high wavenumber 2912 cm⁻¹ to 2970 cm⁻¹, these peaks assigned to the C-H stretching mode [30]. After the inclusion of La₂O₃ nanoparticles, the strong peak at 609 cm⁻¹ was shifted to 611 cm⁻¹. The La₂O₃ nanoparticles interact with the chlorine atoms in the PVC chain through electrostatic forces or weak chemical bonding. This interaction slightly alters the vibrational energy of the C-Cl bond, causing the peak to shift to a higher wavenumber (611 cm⁻¹).

A new absorption band at 856 cm⁻¹ appeared in samples containing 2 and 3 wt% La₂O₃ which is assigned to C-O bending vibrations. In addition, there is another new absorption band at around 417 cm⁻¹ presented in all samples containing different weights of La₂O₃ due to La-O bending [31]. Final observation the absorption band at 1064 cm⁻¹ increased with increasing the content of the La₂O₃ into the PVC films. These outcomes illustrated the interaction between La₂O₃ and PVC in the form of polymer nanocomposites film. La₂O₃ form weak chemical bonds with the carbon atoms in the PVC chain, altering the vibrational energy of the C-C bond and leading to a stronger absorption signal.

It is observed that the nanocomposite films exhibit a small shift in peak position towards higher wave numbers with an increase in La₂O₃ content (0.3–1.0 wt%). However, the FTIR spectra do not show any absorption band associated with La₂O₃, and the positions of all peaks change slightly due to the low content of La₂O₃ nanoparticles. Analysis using complementary techniques such as X-ray diffraction (Fig. 1) or scanning electron microscopy (SEM) could provide additional insights into the structure and incorporation of the nanocomposite materials with PVC matrix. Therefore, these outcomes from FTIR and in combination with the XRD results, indicate the interaction between PVC and La₂O₃ in the polymer nanocomposite films.

Raman Spectroscopy is a practical and efficient method to characterize the structure of nanocomposites materials. The Raman spectra of pure PVC and PVC-La₂O₃ with different content are shown in Fig. 3. The Raman spectra analysis of pure PVC exhibited characteristic bands attributed to specific vibrational modes. The spectral region between

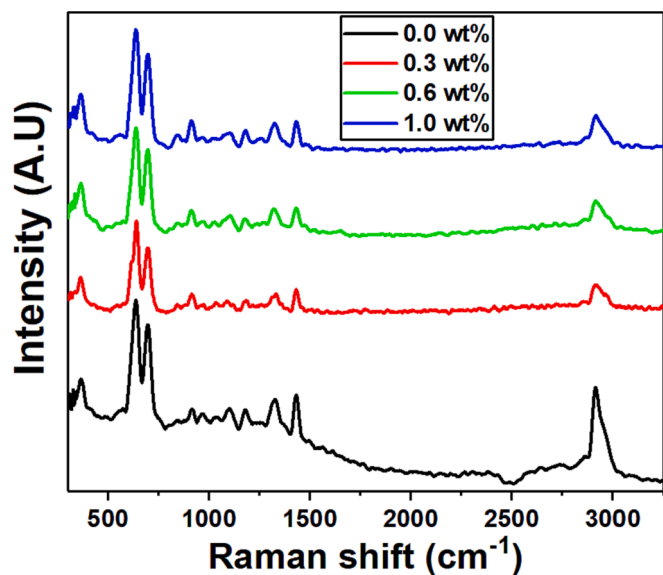


Fig. 3. Raman spectra of pure PVC and PVC-La₂O₃ nanocomposites with different concentration.

630 and 690 cm⁻¹ was assigned to the (C-Cl) stretching vibrations [32], whereas the band observed in the range of 1328 to 1432 cm⁻¹ was associated with the CH₂ scissors vibration. Additionally, the Raman band at 2914 cm⁻¹ corresponds to the (C-H) stretching mode in the pure PVC sample [33,34]. The results showed that the intensity signals of PVC-La₂O₃ blend had decreased in comparison to that of the pure PVC spectra. This can be attributed to the complexing of nanoparticles into the polymer matrix, resulting in a decrease in the regularity of PVC upon the incorporation of La₂O₃. The La₂O₃ particles might be interacting

with the PVC chains, restricting their vibrational freedom, and leading to a weaker (C-H) stretching signal. This provides strong evidence of the successful loading of La₂O₃ metal oxides on the PVC surface.

The SEM surface morphology of polymer films was studied using an environmental scanning electron microscope (ESEM). The SEM micrographs for PVC/La₂O₃ nanocomposite films are given in Fig. 4a-d. All the polymer films showed a smooth surface morphology. Moreover, the scans of polymer films revealed homogeneous distribution of La₂O₃ nanofillers.

Optical absorption spectra of polymer films provide several benefits for studying their properties. Firstly, they allow for the investigation of the optical properties of the films, such as absorption and transmission spectra, absorption coefficient, and energy gap [35]. These properties provide insights into the electronic structure and energy levels of the polymers, which are important for understanding their behaviour in various applications [36]. Additionally, optical absorption spectra can be used to determine the dielectric constant of the films, which is crucial for characterizing their electrical properties [37]. Fig. 5a,b show the results of absorbance and transmittance for the PVC/La₂O₃ films in the spectral region of 200–1000 nm. A band of absorption at 280 nm was visible in the spectra of PVC film that is produced by the $\pi \rightarrow \pi^*$ transitions of unsaturated C=O and C=C [28].

Increasing the content of La₂O₃ in the PVC polymer film led to a red shift in the absorption edge. The red shift indicates interactions between the nanofiller and the polymer matrix, leading to the formation of charge transfer and improved crystallinity of the hybrid polymer nanocomposites [38]. The addition of La₂O₃ nanoparticles to polymer films leads to a decrease in transmittance at specific wavelengths, resulting in enhanced optical properties. This decrease in transmittance can be advantageous for applications that require controlled light transmission, such as optical devices [39]. The decrease in optical transmittance of polymer films with increasing content of nanofiller can be attributed to increased light scattering within the film because of

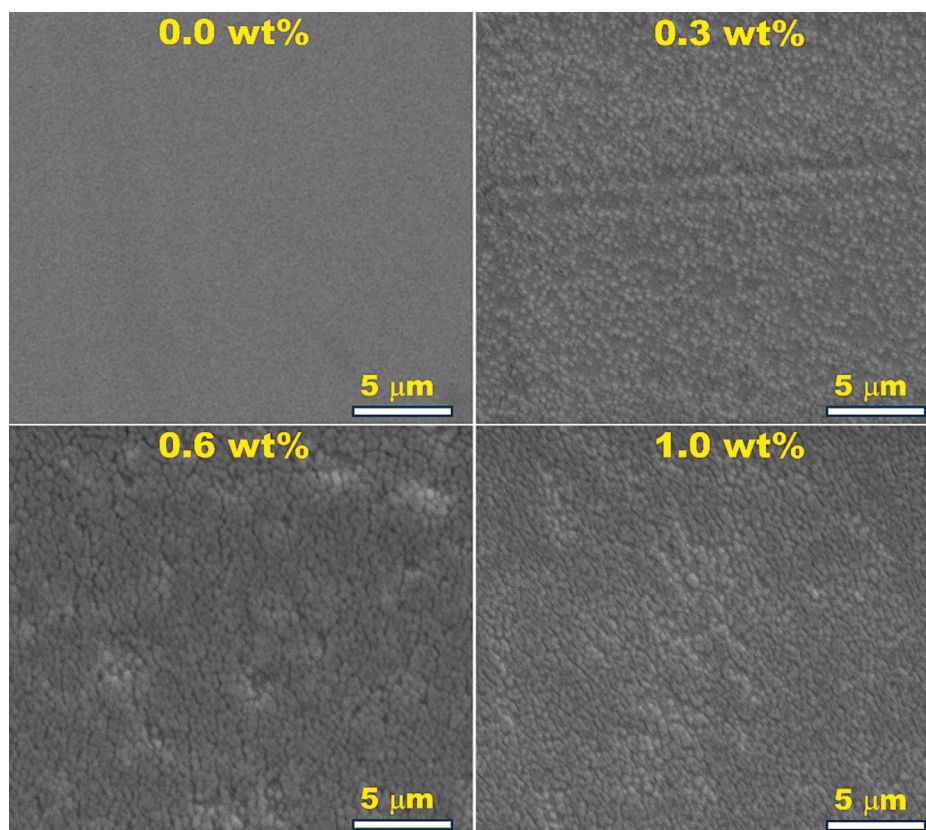


Fig. 4. ESEM micrographs for the PVC/La₂O₃ films.

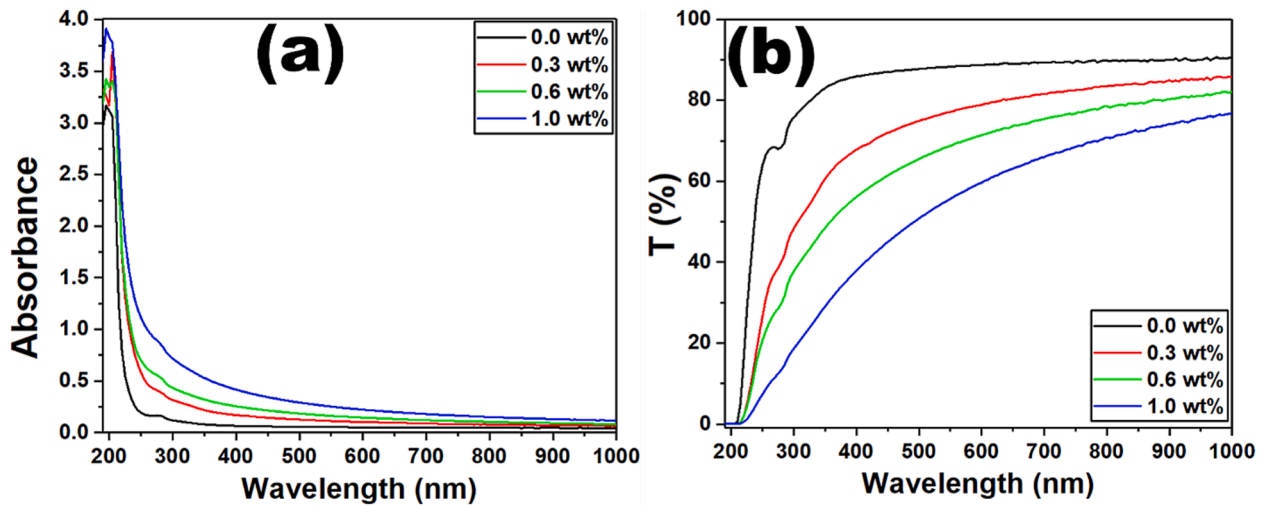


Fig. 5. Plots of (a) absorbance and (b) transmittance for the PVC/La₂O₃ films.

development of molecular complexes between the polymer and the filler [40].

The band gap values of manufactured polymer composites may be changed by varying the amount and type of nanofiller. The Tauc equation is commonly used for determining the optical band gap and electronic transitions within the band gap of polymer film materials. Therefore, Tauc analysis is used to calculate the optical band gap by extrapolating the linear section of the Tauc's plot. [41,42];

$$\alpha h\nu = B(h\nu - E_g)^n \tag{2}$$

where α represents the absorption coefficient, $h\nu$ stands for the energy of the incident photons, and B represents a constant. The values of n determine the type of optical transitions, where $n = 0.5$ for direct allowed transitions. However, $n = 2$ for indirect allowed transitions. As illustrated in Fig. 6a,b, these values are obtained by extrapolating the linear portion close to the beginning of the absorption edge to cross the energy axis.

The obtained band gaps ($E_{g(ind)}$ and $E_{g(dir)}$) are listed in Table 1. The presence of La₂O₃ nanofillers leads to the development of molecular complexes between the polymer matrix and the filler, as indicated by FTIR analysis. This interaction results in modifications in the electronic structure of the polymer, leading to a decrease in the energy gap [38]. The presence of La₂O₃ nanofillers in PVC polymer matrix leads to the formation of localized electronic states, acting as trapping and recombination centres, resulting in a change in the optical band gap. This change can also be attributed to an increase in disorder caused by alterations in the polymer structure [43].

Table 1
Optical parameters of PVC/La₂O₃ polymer films.

La ₂ O ₃ (wt%)	E _{g(ind)} (eV)	E _{g(dir)} (eV)	E ₀ (eV)	E _d (eV)	n ₀
0.0	5.46	5.72	5.88	5.64	1.40
0.3	5.33	5.54	3.92	5.13	1.52
0.6	5.23	5.46	3.69	6.22	1.64
1.0	5.0	5.37	3.28	7.20	1.79

Studying the refractive index of polymer films offers several benefits. The optical and electrical performance of high refractive index polymer films has been the subject of investigation in optoelectronic applications. The refractive index of a polymer film is influenced by factors such as molecular structure, dopants, film thickness, and stretching [44]. Reflectance is a measure of the amount of light that is reflected from a surface. We have estimated the reflectance through the equation ($R = 1 - \sqrt{Te^A}$). The variation of reflectance versus wavelength at different content of La₂O₃ is displayed in Fig. 7a. The relation between reflectance (R) and refractive index (n) can be determined using the following equation [45,46];

$$n = \left(\frac{1+R}{1-R} \right) + \sqrt{\frac{4R}{(1-R)^2} - k^2} \tag{3}$$

where ($k = \alpha\lambda/4\pi$) stands for the extinction coefficient. The refractive index rises in direct proportion to the increase in La₂O₃ content, as seen in Fig. 7b. This densification of nanocomposite films results from the

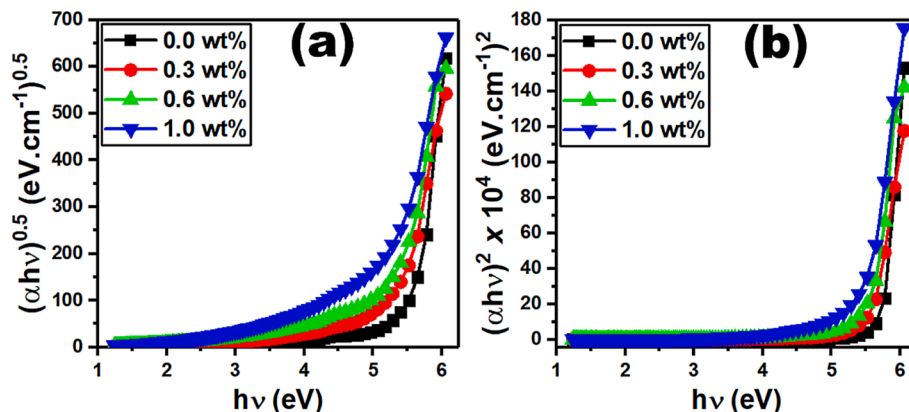


Fig. 6. Variations of (a) $(\alpha h \nu)^{0.5}$ and (b) $(\alpha h \nu)^2$ vs. $h \nu$ for the PVC/La₂O₃ films.

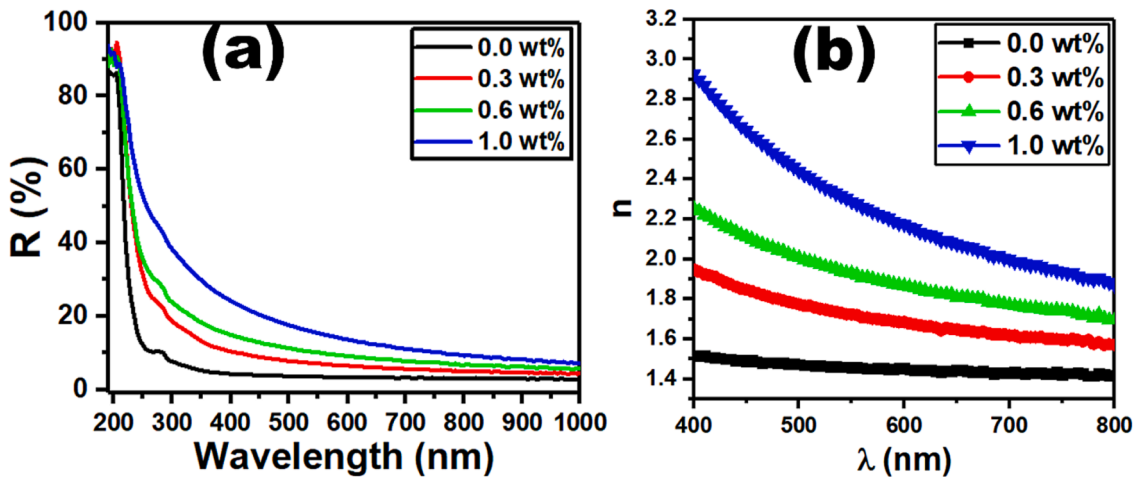


Fig. 7. Variation of (a) reflectance (R) and (b) refractive index vs. wavelength for the PVC/La₂O₃ films.

combination of small La₂O₃ nanoparticles into a large cluster [47]. The possible applications of a high-refractive-index polymer film include optical coatings, anti-reflection coatings, and optical devices. The refractive index enhancement of polymers can be used in applications such as reflectors and nanophotonic systems [48].

The single oscillator model proposed by Wemple and DiDomenico estimates the dispersion parameters of the material, such as oscillator energy, dispersion energy, and transition moments, which are essential for calculating the refractive index [49]. The refractive dispersion includes the single-oscillator energy (E_0) and dispersion energy (E_d) which are calculated from the single oscillator model which proposed by Wemple and DiDomenico [50];

$$(n^2 - 1)^{-1} = \frac{E_0}{E_d} - \frac{1}{E_0 E_d} (h\nu)^2 \quad (4)$$

The slope and intercept of the $(n^2 - 1)^{-1}$ versus $(h\nu)^2$ plots located in Fig. 8a were used to determine the values of E_0 and E_d . The obtained values of E_0 showed a decrease (5.88 – 3.28 eV) while E_d increases (5.64 – 7.20 eV) upon increasing the concentration of La₂O₃ nanofiller (see Table 1). The increase in dispersion energy in a polymer film is attributed to increased polymer chain packing during orientation, leading to enhanced intermolecular interactions [51]. Moreover, the long-range van der Waals or dispersion force can amplify thermal fluctuations in thin polymer films, leading to an increase in dispersion energy [52].

The static refractive index (n_0) of a polymer can be determined using

the single oscillator model proposed by Wemple and DiDomenico at zero photon energy ($h\nu = 0$) as follows [53];

$$n_0^2 = \left(1 + \frac{E_d}{E_0} \right) \quad (5)$$

The estimated values of n_0 showed an increase (1.40 – 1.79) upon increasing the percentage of La₂O₃ nanofiller. High refractive index polymers offer promise for usage in a variety of optoelectronic devices. These applications include complex display devices, where they can be employed to improve performance, as well as light-emitting diode encapsulants. They can also be used in the fabrication of plastic lenses for eyeglasses [54]. Therefore, the addition of La₂O₃ nanofiller improved the refractive index of polymer films and thus allows for better performance in optical applications such as micro lenses, image sensors, and organic light-emitting diodes [55].

The recommended optical transitions are determined via the real band gap (E_r) that can be obtained by extrapolating the linear part near the onset of the absorption edge to the intersection of the optical dielectric loss ($\epsilon_2 = 2nk$ [56]). The plots of ϵ_2 versus $h\nu$ for the PVC/La₂O₃ films are displayed in Fig. 8b. The calculations revealed the values recorded in Table 2 which is close to the $E_{g(\text{dir})}$. Therefore, the major optical transitions occur in the PVC/La₂O₃ films are the direct transitions.

The oscillator strength (f) of a polymer film can be affected by several factors, including the chemical structure of the polymer, the molecular

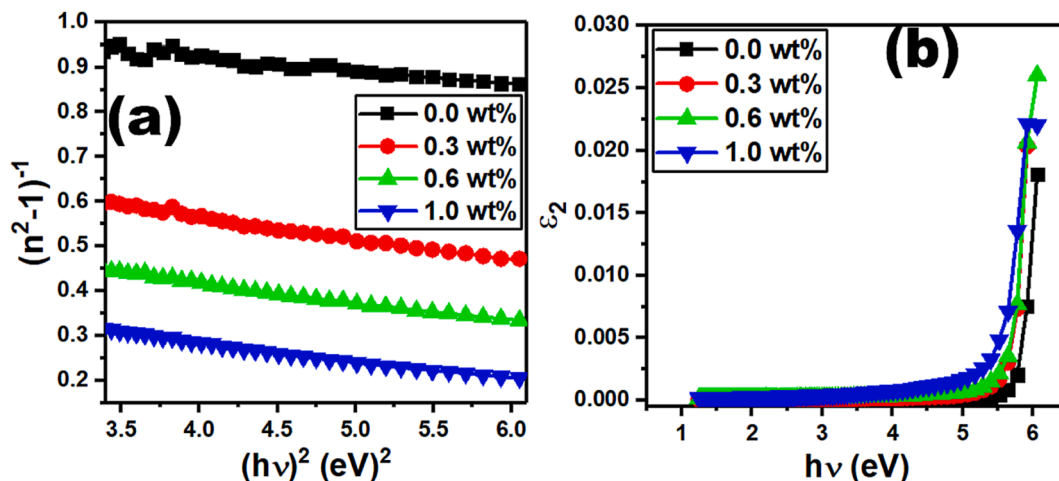


Fig. 8. Variation of (a) $(n^2 - 1)^{-1}$ vs. $(h\nu)^2$, and (b) ϵ_2 vs. $h\nu$ for the PVC/La₂O₃ films.

Table 2
Dispersion parameters PVC/La₂O₃ polymer films.

La ₂ O ₃ (wt %)	f (eV ²)	$\chi^{(1)}$ (esu)	$\chi^{(3)} \times 10^{-15}$ (esu)	$n_2 \times 10^{-13}$ (esu)	E_r (eV)
0.0	33.21	0.08	5.77	1.56	5.77
0.3	20.15	0.10	19.97	4.96	5.70
0.6	22.91	0.13	55.20	12.70	5.66
1.0	23.58	0.17	159.22	33.56	5.54

weight of the polymer, the film thickness, and the aggregation of the polymer molecules. The oscillator strength of a polymer film is an important parameter for several applications, such as organic solar cells, light-emitting diodes, and lasers. By understanding the factors that affect the oscillator strength, it is possible to design polymers with the desired optical properties for these applications. The oscillator strength can be calculated using the following equation [57]:

$$f = E_d E_0 \quad (6)$$

The data of oscillator strength are given in Table 2. The addition of La₂O₃ nanofillers decreased the oscillator strength of a polymer film.

The electronic structure of molecules in polymer films is intricately linked to their underlying chemical structure, thereby influencing the linear and nonlinear optical susceptibilities. These susceptibilities play a pivotal role in various applications, including optical data storage, optical switching, and the development of nonlinear optical devices. Hence, understanding and characterizing the linear and nonlinear optical susceptibilities of polymer films become essential for leveraging their potential in these technological domains [58]. The linear optical susceptibility ($\chi^{(1)}$) and third-order nonlinear optical susceptibility ($\chi^{(3)}$) of polymer films can be calculated using the following equations [59]:

$$\chi^{(1)} = \frac{E_d/E_0}{4\pi}, \chi^{(3)} = 6.82 \times 10^{-15} (E_d/E_0)^4 \quad (8)$$

The estimated values of ($\chi^{(1)}$) and ($\chi^{(3)}$) are listed in Table 2 for PVC/La₂O₃ polymer films. The nanofillers can enhance the local electric field at the polymer-nanofiller interface, which can increase the third-order nonlinear optical susceptibility. Moreover, the nanofillers can interact with the polymer molecules and form new energy levels, which can also increase the third-order nonlinear optical susceptibility [60]. The nonlinear refractive index (n_2) of a polymer film can be affected by the chemical structure of the polymer molecules that determines the polarizability of the molecules, which in turn affects the nonlinear refractive index [61]. The nonlinear refractive index of polymer films is an important parameter for a variety of applications, such as optical limiters, optical switches, and optical data storage [62]. The following equation is used for the calculation of nonlinear refractive index (n_2) [63];

$$n_2 = \frac{12\pi\chi^{(3)}}{n_0} \quad (9)$$

The data estimated for n_2 were recorded in Table 2. The addition of La₂O₃ nanofillers increase the polarizability of the polymer molecules and hence the nonlinear refractive index. This enhancement is attributed to the strong interfacial interactions between the nanofiller particles and the polymer matrix, which cause a distortion of the electron cloud around the polymer molecules. This distortion, in turn, increases the susceptibility of the polymer to electric fields, leading to an increase in the nonlinear optical properties of the material [64]. The improvement of the nonlinear refractive index of polymer films is a promising area of application. By improving the nonlinear refractive index, it is possible to develop polymer films with even better optical properties for a variety of applications.

Conclusions

In-depth analysis and discussion have been conducted on the impact of La₂O₃ inclusion on the structural, physical, linear, and non-linear optical characteristics of PVC polymer films. The crystal structure of La₂O₃ was confirmed as hexagonal phase from XRD analysis. The La₂O₃ nanostructure was found to have crystallites size with an average about 15 nm. The obtained band gaps of PVC/La₂O₃ polymer nanocomposites decreased upon increasing the nanofiller content. The obtained values of E_0 showed a decrease (5.88 – 3.28 eV) while E_d increases (5.64 – 7.20 eV) upon increasing the concentration of La₂O₃. The estimated values of n_0 showed an increase (1.40 – 1.79) upon increasing the percentage of La₂O₃. Finally, the addition of La₂O₃ nanofillers increase the polarizability of the polymer molecules and hence the nonlinear refractive index.

Compliance with ethical standards

Yes, this paper complies with the journal's ethical guidelines.

Research data policy and Data Availability statements

On reasonable request, the author will make the datasets created during and/or analyzed during the current investigation.

Authors contributions

All the authors have contributed equally.

Funding

The authors extend their appreciation to the Deputyship for Research & Innovation, Ministry of Education in Saudi Arabia for funding this research work through the project number 223202.

CRediT authorship contribution statement

Sultan Alhassan: Writing – review & editing, Writing – original draft, Investigation. **Khulaif Alshammari:** Writing – review & editing, Investigation, Formal analysis. **Majed Alshammari:** Writing – review & editing, Visualization. **Turki Alotaibi:** Writing – original draft, Conceptualization. **Alhulw H. Alshammari:** Writing – review & editing, Methodology, Conceptualization. **Ali Alhamazani:** Investigation, Conceptualization. **Mohamed Henini:** Writing – review & editing, Supervision. **Taha Abdel Mohaymen Taha:** .

Declaration of competing interest

The authors declare that they have no known competing financial interests or personal relationships that could have appeared to influence the work reported in this paper.

Data availability

Data will be made available on request.

Acknowledgments

The authors gratefully acknowledge the central lab at Jouf University for providing the advance experiments methods used in this manuscript.

References

- [1] Wei H, Wang H, Li A, Cui D, Zhao Z, Chu L, et al. Multifunctions of polymer nanocomposites: environmental remediation, electromagnetic interference shielding, and sensing applications. *ChemNanoMat* 2020;6(2):174–84.

- [2] Gong M, Zhang L, Wan P. Polymer nanocomposite meshes for flexible electronic devices. *Prog Polym Sci* 2020;107:101279.
- [3] Saleh TA, Parthasarathy P, Irfan M. Advanced functional polymer nanocomposites and their use in water ultra-purification. *Trends Environ Anal Chem* 2019;24:e00067.
- [4] Wu H, Fahy WP, Kim S, Kim H, Zhao N, Pilato L, et al. Recent developments in polymers/polymer nanocomposites for additive manufacturing. *Prog Mater Sci* 2020;111:100638.
- [5] Luo X, Cheng H, Wu X. Nanomaterials reinforced polymer filament for fused deposition modeling: a state-of-the-art review. *Polymers* 2023;15(14):2980.
- [6] Habashy MM, Abd-Elhady AM, Elsad RA, Izzularab MA. Performance of PVC/SiO₂ nanocomposites under thermal ageing. *Appl Nanosci* 2021;11(7):2143–51.
- [7] Xie XL, Liu QX, Li RKY, Zhou XP, Zhang QX, Yu ZZ, et al. Rheological and mechanical properties of PVC/CaCO₃ nanocomposites prepared by in situ polymerization. *Polymer* 2004;45(19):6665–73.
- [8] Ramesh S, Winie T, Arof AK. Investigation of mechanical properties of polyvinyl chloride–polyethylene oxide (PVC–PEO) based polymer electrolytes for lithium polymer cells. *Eur Polym J* 2007;43(5):1963–8.
- [9] Al Naim A, Alnaim N, Ibrahim SS, Metwally SM. Effect of gamma irradiation on the mechanical properties 362 of PVC/ZnO polymer nanocomposite. *J Radiat Res Appl Sci* 2017;10(3):165–71.
- [10] Wang D, Wilkie CA. Preparation of PVC-clay nanocomposites by solution blending. *J Vinyl Add Tech* 2002;8(4):238–45.
- [11] Hasan M, Lee M. Enhancement of the thermo-mechanical properties and efficacy of mixing technique in the preparation of graphene/PVC nanocomposites compared to carbon nanotubes/PVC. *Prog Nat Sci: Mater Int* 2014;24(6):579–87.
- [12] Sadek EM, Mansour NA, Ahmed SM, Abd-El-Messieh SL, El-Komy D. Synthesis, characterization and applications of poly (vinyl chloride) nanocomposites loaded with metal oxide nanoparticles. *Polym Bull* 2021;78:5481–502.
- [13] Ebnalwaled AA, Thabet A. Controlling the optical constants of PVC nanocomposite films for optoelectronic applications. *Synth Met* 2016;220:374–83.
- [14] Hasan M, Banerjee AN, Lee M. Enhanced thermo-mechanical performance and strain-induced band gap reduction of TiO₂@ PVC nanocomposite films. *Bull Mater Sci* 2015;38:283–90.
- [15] Gholami A, Moghadassi AR, Hosseini SM, et al. Preparation and characterization of polyvinyl chloride based nanocomposite nanofiltration-membrane modified by iron oxide nanoparticles for lead removal from water. *J Ind Eng Chem* 2014;20:1517–22.
- [16] Zhang D, Li Z, Gao F, Wei X, Ni Y. Tribological performance of polymer composite coatings modified with La₂O₃ and MoS₂ nanoparticles. *J Tribol* 2019;141(11):111601.
- [17] Sharma SP, Dwivedi DK, Jain PK. Effect of La₂O₃ Addition on the Microstructure, Hardness and Abrasive Wear Behavior of Flame Sprayed Ni Based Coatings. *Wear* 2009;267(5):853–9.
- [18] Pathan AA, Desai KR, Bhasin CP. Synthesis of La₂O₃ nanoparticles using glutaric acid and propylene glycol for future CMOS applications. *Int J Nanomater Chem* 2017;3:21–5.
- [19] Mutharani B, Ranganathan P, Chen SM, Karuppiah C. Simultaneous voltammetric determination of acetaminophen, naproxen, and theophylline using an in-situ polymerized poly (acrylic acid) nanogel covalently grafted onto a carbon black/La₂O₃ composite. *Microchim Acta* 2019;186:1–11.
- [20] Fan L, Yu L, Xu F, Qin G, Chen Q. Preparation of PVA-based composite alkaline solid polymer electrolyte with La₂O₃ nanoparticle filler. *J Nanopart Res* 2021;23:1–9.
- [21] Song J, Lu C, Xu D, Ni Y, Liu Y, Xu Z, et al. The effect of lanthanum oxide (La₂O₃) on the structure and crystallization of poly (vinylidene fluoride). *Polym Int* 2010;59(7):954–60.
- [22] Ramesh S, Chai MF. Conductivity, dielectric behavior and FTIR studies of high molecular weight poly (vinylchloride)–lithium triflate polymer electrolytes. *Mater Sci Eng B* 2007;139(2–3):240–5.
- [23] Hassen MM, Ibrahim IM, Abdullah OG, Suhail MH. Improving photodetector performance of PANI nanofiber by adding rare-earth La₂O₃ nanoparticles. *Appl Phys A* 2023;129(2):135.
- [24] Khound S, Sarmah JK, Sarma R. Hybrid La₂O₃-cPVP dielectric for organic thin film transistor applications. *ECS J Solid State Sci Technol* 2022;11(1):013007.
- [25] Hodge IM. Effects of annealing and prior history on enthalpy relaxation in glassy polymers. 4. Comparison of five polymers. *Macromolecules* 1983;16(6):898–902.
- [26] Alshammari AH, Alshammari M, Ibrahim M, Alshammari K, Taha TAM. Processing polymer film nanocomposites of polyvinyl chloride–Polyvinylpyrrolidone and MoO₃ for optoelectronic applications. *Opt Laser Technol* 2024;168:109833.
- [27] Alshammari M, Alhassan S, Alshammari K, Alotaibi T, Alshammari AH, Alotibi S, et al. Hydrogen catalytic performance of hybrid Fe₃O₄/FeS₂/g-C₃N₄ nanocomposite structures. *Diam Relat Mater* 2023;138:110214.
- [28] Taha TA, Saleh A. Dynamic mechanical and optical characterization of PVC/fGO polymer nanocomposites. *Appl Phys A* 2018;124(9):600.
- [29] Solodovnichenko VS, Polyboyarov VA, Zhdanok AA, Arbizov AB, Zapevalova ES, Kryazhev YG, et al. Synthesis of carbon materials by the short-term thermochemical activation of polyvinyl chloride. *Procedia Eng* 2016;152:747–52.
- [30] Pandey M, Joshi GM, Mukherjee A, Thomas P. Electrical properties and thermal degradation of poly (vinyl chloride)/polyvinylidene fluoride/ZnO polymer nanocomposites. *Polym Int* 2016;65(9):1098–106.
- [31] Shafira H, Yunarti RT, Saefumillah A. Development Study of Binding Agent in Diffusive Gradient In Thin Films (DGT) Technique for Absorption of Phosphate Compounds using Nano-La₂O₃. *Jurnal Kimia VALENSI* 2022;8(2):280–8.
- [32] Taha TA, Ismail Z, Elhawary MM. Structural, optical and thermal characterization of PVC/SnO₂ nanocomposites. *Appl Phys A* 2018;124(4):307.
- [33] Conradi M, et al. Mechanical properties of high density packed silica/poly(vinyl chloride) composites. *Polym Eng Sci* 2013;53(7):1448–53.
- [34] Shari'ati Y, Vura-Weis J. Polymer thin films as universal substrates for extreme ultraviolet absorption spectroscopy of molecular transition metal complexes. *J Synchrotron Radiat* 2021;28(6):1850–7.
- [35] Hajduk B, Bednarski H, Trzebiecka B. Temperature-dependent spectroscopic ellipsometry of thin polymer films. *J Phys Chem B* 2020;124(16):3229–51.
- [36] Imad, Al, Deen, Hussein, Ali, Al, Saidi., Hussein, Fali, Hussein., Numan, Sleem, Hashim. (2020). Preparation of Poly(3HT - Co - TH) - PMMA Polymer Blend Films and Study Their Optical Properties. *Int J Eng Trends Technol*, 68(12):72–6.
- [37] Dongkyun S, Jonghyup P, Tae JS, Pil JY, Juhyun P, Kyungwon K. Bathochromic shift in absorption spectra of conjugated polymer nanoparticles with displacement along backbones. *Macromol Res* 2015;23(6):574–7.
- [38] Haider M, Shanshool Muhammad, Yahaya Wan, Mahmood Mat, Yunus Ibtisam, Yahya Abdullah, Ibtisam Abdullah Yahya. Investigation of energy band gap in polymer/ZnO nanocomposites. *J Mater Sci Mater Electron* 2016;27(9):9804–11.
- [39] Muthupandeewari A, Kalyani P, Nehru LC. On the effects of high loading of ZnO nanofiller on the structural, optical, impedance and dielectric features of PVA@ ZnO nanocomposite films. *Polym Bull* 2021;78(12):1–18. <https://doi.org/10.1007/S00289-020-03443-6>.
- [40] Heiba ZK, Mohamed MB, Ahmed SI. Exploring the physical properties of PVA/PEG polymeric material upon doping with nano gadolinium oxide. *Alex Eng J* 2022;61(5):3375–83.
- [41] Taha TA, Abouhaswa AS. Structure, optical and magnetic properties of barium sulfonium borate/cobalt oxide glass structures. *Opt Quant Electron* 2023;55(6):483.
- [42] Yixuan H, Xinru H, Alan CW, Rohrbach Connie, Roth B. Comparing refractive index and density changes with decreasing film thickness in thin supported films across different polymers. *J Chem Phys* 2020;153(4):044902.
- [43] Abdullah OG, Aziz SB, Omer KM, Salih YM. Reducing the optical band gap of polyvinyl alcohol (PVA) based nanocomposite. *J Mater Sci Mater Electron* 2015; 26:5303–9.
- [44] Alhassan S, Alshammari M, Alshammari K, Alotaibi T, Alshammari AH, Fawaz Y, et al. Preparation and Optical Properties of PVDF-CaFe₂O₄ Polymer Nanocomposite Films. *Polymers* 2023;15(9):2232.
- [45] Alhassan S, Alshammari K, Alshammari M, Alotaibi T, Alshammari AH, Fawaz Y, et al. Synthesis and optical properties of polyvinylidene difluoride nanocomposites comprising MoO₃/g-C₃N₄. *Results Phys* 2023;48:106403.
- [46] El-naggar AM, Heiba ZK, Mohamed MB, Kamal AM, Osman MM, Albassam AA, et al. Improvement of the optical characteristics of PVA/PVP blend with different concentrations of SnS₂/Fe. *J Vinyl Add Tech* 2022;28(1):82–93.
- [47] Yasir M, Sai T, Sicher A, Scheffold F, Steiner U, Wilts BD, et al. Enhancing the Refractive Index of Polymers with a Plant-Based Pigment. *Small* 2021;17(44):2103061.
- [48] Al Orainy RH. Single oscillator model and refractive index dispersion properties of ternary ZnO films by sol gel method. *J Sol-Gel Sci Technol* 2014;70:47–52.
- [49] Štrbac DD, Lukic SR, Dragoslav M, Petrović JM, González-Leal Srinivasan Ashok. Single oscillator energy and dispersion energy of uniform thin chalcogenide films from Cu–As–S–Se system. *J Non Cryst Solids* 2007;353(13):1466–9.
- [50] Stachewicz U, Li S, Bilotti E, Barber AH. Dependence of surface free energy on molecular orientation in polymer films. *Appl Phys Lett* 2012;100(9).
- [51] Dutcher, J. R., Dalnoki-Veress, K., Nickel, B. G., & Roth, C. B. (2000, October). Instabilities in thin polymer films: From pattern formation to rupture. In *Macromolecular Symposia* (Vol. 159, No. 1, pp. 143-150). Weinheim: WILEY-VCH Verlag.
- [52] Taha TA, Hendawy N, El-Rabaie S, Esmat A, El-Mansy MK. Effect of NiO NPs doping on the structure and optical properties of PVC polymer films. *Polym Bull* 2019;76(9):4769–84.
- [53] Tomoya H, Mitsuru U, Mitsuru U. Recent Progress in High Refractive Index Polymers. *Macromolecules* 2015;48(7):1915–29.
- [54] Tang Y, Cabrini S, Nie J, Pina-Hernandez C. High-refractive index acrylate polymers for applications in nanoimprint lithography. *Chin Chem Lett* 2020;31(1):256–60.
- [55] Deshpande MP, Solanki GK, Agarwal MK. Optical band gap in tungsten diselenide single crystals intercalated by indium. *Mater Lett* 2000;43(1–2):66–72.
- [56] Alshammari AH, Alshammari K, Alshammari M, Taha TAM. Structural and optical characterization of g-C₃N₄ nanosheet integrated PVC/PVP polymer nanocomposites. *Polymers* 2023;15(4):871.
- [57] Mondal R, Biswas D, Paul S, Das AS, Chakrabarti C, Roy D, et al. Investigation of microstructural, optical, physical properties and dielectric relaxation process of sulphur incorporated selenium–tellurium ternary glassy systems. *Mater Chem Phys* 2021;257:123793.
- [58] Nalwa HS. Organic materials for third-order nonlinear optics. *Adv Mater* 1993;5(5):341–58.
- [59] Keru G, Ndungu PG, Nyamori VO. A review on carbon nanotube/polymer composites for organic solar cells. *Int J Energy Res* 2014;38(13):1635–53.
- [60] Divya R, Manikandan N, Girisun TS, Vinita G. Investigations on the structural, morphological, linear and third order nonlinear optical properties of manganese doped zinc selenide nanoparticles for optical limiting application. *Opt Mater* 2020; 100:109641.
- [61] Bredas JL, Adant C, Tackx P, Persoons A, Pierce BM. Third-order nonlinear optical response in organic materials: theoretical and experimental aspects. *Chem Rev* 1994;94(1):243–78.

- [62] Innocenzi P, Lebeau B. Organic–inorganic hybrid materials for non-linear optics. *J Mater Chem* 2005;15(35–36):3821–31.
- [63] Dhatarwal P, Sengwa R.J. Investigation on the optical properties of (PVP/PVA)/Al₂O₃ nanocomposite films for green disposable optoelectronics. *Phys B Condens Matter* 2021;613:412989.
- [64] Abdullah OG, Salh DM, Mohamad AH, Jamal GM, Ahmed HT, Mustafa BS, et al. Linear and nonlinear optical characterization of dye–polymer composite films based on methylcellulose incorporated with varying content of methylene blue. *J Electron Mater* 2022;51:675–83.